This is the peer-reviewed, final accepted version for American Mineralogist, published by the Mineralogical Society of America.
The published version is subject to change. Cite as Authors (Year) Title. American Mineralogist, in press.
DOI: https://doi.org/10.2138/am-2023-9197. http://www.minsocam.org/

REVISION 1

Word count: 8,986

Local strain heterogeneity associated with Al/Si ordering in anorthite, $CaAl_2Si_2O_8$, with implications for thermodynamic mixing behaviour and trace element partitioning in plagioclase feldspars

ALISON J. ATKINSON[1], TIZIANA BOFFA BALLARAN[2], AND MICHAEL A. CARPENTER[1]

[1]Dept. Earth Sciences, University of Cambridge, Downing Street, Cambridge CB2 3EQ, U.K.

[2]Bayerisches Geoinstitut, Universität Bayreuth, D-95440 Bayreuth, Germany

ABSTRACT

Hard Mode IR powder absorption spectroscopy has been used to characterise local strain relaxation associated with Al/Si ordering in a suite of synthetic anorthite samples with structural states that vary from a high degree of Al/Si order through a metastable incommensurate structure at intermediate states of order to long range order with $I\bar{1}$ symmetry. The dominant feature accompanying the changing structural states is line broadening, which has been quantified by autocorrelation analysis and is attributed to local heterogeneous strain variations on a length scale of at least 1-5 unit cells. The autocorrelation results are consistent with contributions to the line broadening as being due to order parameters for both the $C\bar{1} \rightarrow I\bar{1}$ and $I\bar{1} \rightarrow P\bar{1}$ transitions which couple biquadratically, $\lambda Q_{\mathrm{od}}^2 Q_{\mathrm{displ}}^2$. Close correlation with enthalpy variations from previously published calorimetric data indicates that the driving force for ordering can be understood in terms of elimination of strain fields arising from accommodating more or less rigid AlO_4 and SiO_4 tetrahedra in the feldspar framework. The metastable

incommensurate structure of anorthite is closely analogous to the stable incommensurate structure that develops at intermediate compositions in the plagioclase solid solution, confirming that the same strain relaxation mechanism dominates the properties and behaviour of all structural states across the solid solution. Elimination of strain heterogeneity by ordering on the basis of $I\bar{1}$ symmetry determines the form of non-ideal mixing shown by the solid solution at high temperatures, and changes in elastic properties may contribute to a break in slope of partitioning of trace elements between crystals and melt.

Keywords: anorthite, Al/Si ordering, hard mode IR spectroscopy, local strain heterogeneity, enthalpy

INTRODUCTION

A number of different strategies have been adopted to describe the thermodynamic properties of plagioclase feldspars in the context of efforts to produce quantitative descriptions of the stability fields of mineral assemblages under the full range of possible geological conditions. Dubacq (2022) summarised contrasting treatments of mixing properties for the $C\bar{1}$ and $I\bar{1}$ structures at high temperatures as those which smooth out the effects of the discrete $C\bar{1} \leftrightarrow I\bar{1}$ transition (Ghiorso 1984; Benisek et al. 2004, 2010; Namur et al. 2012; Holland et al. 2022), those which treat states with different symmetries as separate solid solutions (Holland and Powell 1992) and those which treat the mixing properties in terms of an Al/Si order/disorder process at anorthite-rich compositions (Carpenter and Ferry 1984; Carpenter 1992, 1994). The differences revolve, in effect, around the need (or otherwise) to include a physically correct description of the phase transition approximately half way across the solid solution. This debate continues because mean field models of Al/Si ordering to give the symmetry change explicitly, such as from Landau theory, do not readily yield equations that can conveniently be incorporated into mixing models with a limited number of variable parameters. As a

consequence, activity-composition descriptions based on conventional asymmetric mixing models are used for applications in petrology, while models based on atomic interactions are used to understand Al/Si ordering at a more fundamental level for albite, anorthite and the more complex incommensurate structures that develop at intermediate compositions during slow cooling in nature.

A significant recent advance in the context of understanding the stability of plagioclase feldspars from an atomic perspective has been provided by a Monte Carlo simulation by Dubacq (2022) which focussed on interactions between nearest neighbour and next nearest neighbour tetrahedral cations. This author concluded that superposition of $I\bar{1}$ ordering on a $C\bar{1}$ solid solution, with large ordering energies for anorthite, can provide reliable results in terms of energy and ordering across the solid solution. However, he also drew attention to the fact that pairwise interaction models, such as used for the Monte Carlo simulation, do not include the contribution of strain fields explicitly. If local strain fields are less than the size of the supercell used in the model they are included implicitly but if they are on a longer length scale they are not. This is a conundrum in all energetic modelling of crystal structures and the present paper is intended to shed light on the influence of local strain effects from an experimental point of view by analysing line broadening in IR absorption spectra.

The generalised result attributed to Eshelby (1957) that a strain field will decay through a medium in three dimensions according to $1/r^3$, where r is distance, implies that placing a specific limit on the length scale of strain fields in a crystal is arbitrary. The expectation is at least that they extend further than nearest or next nearest neighbour atoms, and there are experimental observations which confirm this view for silicates. For example, diffraction contrast in a transmission electron microscope image of exsolution of augite from pigeonite shows a strain field extending up to ~250 Å from the tip of an augite precipitate (Carpenter 2002). Similarly, Figure 7.10 of Salje (1993) shows that the strain field from a kink of individual domain wall in KAl_3SiO_8 can influence the topology of adjacent walls at distances of ~1,000 Å. In a different context, the extent of the plateau of transition temperature as a function of composition towards $KAlSi_3O_8$ for the displacive transition temperature near ~1325 K in

This is the peer-reviewed, final accepted version for American Mineralogist, published by the Mineralogical Society of America.
The published version is subject to change. Cite as Authors (Year) Title. American Mineralogist, in press.
DOI: https://doi.org/10.2138/am-2023-9197. http://www.minsocam.org/

albite, $NaAlSi_3O_8$, implies that the effective strain field around K^+ has a diameter of 20-40 Å (Carpenter et al. 1999). Length scales of 10's of Å overlap with estimates of the length scales of phonons that are sampled in vibrational spectroscopy. The sensitivity of phonons to all the structural variations in natural plagioclase crystals is seen in Raman spectra, for example (Bersani et al. 2018). According to Atkinson et al. (1999) for feldspars, phonon length scales of 2-5 Å at 1500 cm^{-1} would become ~8-25 Å at 500 cm^{-1} and ~60-150 Å at 50 cm^{-1}. The essential point is that phonon spectroscopy provides, in principle, a probe with the correct length scale to detect and characterise structural heterogeneity related to local strain relaxation in silicates.

The present study follows on from the Hard Mode IR powder absorption spectroscopy study of local structural heterogeneity in natural and heat treated plagioclase feldspars by Atkinson et al. (1999). It was designed to take advantage of a suite of synthetic anorthite samples prepared with a sequence of metastable structural states starting from a high degree of Al/Si disorder, through incommensurate states with intermediate degrees of order to the equilibrium state with ordering based on $I\bar{1}$ symmetry. A key advantage of this suite is that the composition is fixed ($CaAl_2Si_2O_8$) and, hence, that all changes in spectral, physical and thermodynamic properties are due directly or indirectly to changes in Al/Si order alone.

EXPERIMENTAL METHODS

Synthesis and characterisation

The two series of synthetic anorthite samples used in the present study were selected from a larger suite of samples crystallised by heating glass of anorthite composition in air (Carpenter 1991a, 1991b, 1992). The first, referred to as a kinetic series, consisted of eight samples with crystallisation times ranging from 1 minute to 17 days at 1400 °C. The second, referred to as an equilibrium series, consisted of six samples equilibrated at temperatures between 850 °C and 1540 °C. A sample crystallised at 1100 °C for 15 minutes, ANC19, has been used as a reference state for maximum

This is the peer-reviewed, final accepted version for American Mineralogist, published by the Mineralogical Society of America.
The published version is subject to change. Cite as Authors (Year) Title. American Mineralogist, in press.
DOI: https://doi.org/10.2138/am-2023-9197. http://www.minsocam.org/

disorder of Al and Si. Times and temperatures for the original synthesis conditions are listed in Table 1, together with details of structural states characterised by transmission electron microscopy, powder X-ray diffraction and high temperature solution calorimetry (from Carpenter 1991a, 1991b, 1992).

The synthetic crystals all contained submicroscopic twinning parallel to (010) on the basis of albite and Carlsbad twin laws (Carpenter 1991a, Xu et al. 1997). The presence of type-e and/or type-b reflections in electron diffraction patterns defined whether the Al/Si order scheme was incommensurate or had evolved through to the commensurate $I\bar{1}$ state. Spacings and orientations of pairs of e-reflections in samples from the kinetic series initially resembled the pattern seen in natural plagioclase samples with the e_2 structure, starting at composition ~An_{30} and evolving continuously through to the pattern for crystals with composition ~An_{55}. With further annealing, the spacing between e-reflections increased, but without further changes in orientation: ~25 Å for ANC19, ~30 Å for ANC60, extending to ~90 Å for ANC73. Evolution of the microstructure was then of type-b antiphase domains with dimensions increasing from ~200 Å in ANC73 Å to ~1,550 in ANC35. The size of type-b antiphase domains in crystals from the equilibrium series was in the range ~2,000-3,000 Å, but was not determined for ANC74/H2.

Diffuse type-c reflections arising from the $I\bar{1} \rightarrow P\bar{1}$ transition were present in diffraction patterns from all the samples, and type-d reflections were seen in diffraction patterns from the most ordered samples. The type-c and type-d reflections were sharp in diffraction patterns from ANC74/H2, which had been prepared initially by crystallisation from glass in air at 1400 °C and then annealed in the presence of water at 850 °C (Carpenter 1992). This treatment resulted in the highest degree of Al/Si order of all the samples listed in Table 1.

Macroscopic distortion of the structure due to Al/Si ordering was quantified in terms of the scalar strain, ε_s (Carpenter 1991b, 1992). Values were determined by first calculating six individual strain components, e_1-e_6, from changes in room temperature lattice parameters of each sample with respect to ANC19 as the reference state (e_1-e_6 = 0) and then diagonalising the strain matrix to determine three

This is the peer-reviewed, final accepted version for American Mineralogist, published by the Mineralogical Society of America.
The published version is subject to change. Cite as Authors (Year) Title. American Mineralogist, in press.
DOI: https://doi.org/10.2138/am-2023-9197. http://www.minsocam.org/

126 principal strains ε_1 - ε_3 (Carpenter et al. 1990). The scalar strain was given by $\varepsilon_s = \sqrt{\sum_{1-3} \varepsilon_i^2}$

127 andincreased with increasing degree of Al/Si order. ΔH_{soln} is the enthalpy of solution in lead borate flux
128 at 700 °C (Carpenter 1991b, 1992). Samples with the lowest enthalpy (most ordered) have the largest
129 values of ΔH_{soln}.

130

131 **Powder absorption infrared spectroscopy**

132 Preparation of pellets used for powder absorption infrared spectroscopy measurements in the present
133 study followed the procedure set out in detail in Atkinson et al. (1999). This involved a carefully
134 repeated pattern of grinding the samples for 20 minutes in an agate ball mortar using a Spex microball
135 mill, mixing in fixed proportions with CsI or polyethylene powder as the matrix phase and pressing
136 under vacuum. CsI pellets weighed 300 mg and contained a ratio of sample to matrix of 1:450.
137 Polyethylene pellets weighed 100 mg and contained a mixture of sample to matrix in the ratio 1:50.

138 Primary spectra were collected under vacuum at room temperature using a Bruker 113V FT-IR
139 spectrometer and a Bruker 66V FT-IR spectrometer. Each spectrum was calculated by Fourier
140 transformation of 512 interferometer scans and recorded as absorbance, $a = -\log_{10}(I_{sample}/I_{reference})$,
141 where I is the single beam transmission intensity. The frequency ranges for spectra from the CsI pellets
142 were 150-700 cm^{-1} and 400-2000 cm^{-1}, with an instrumental resolution of 2 cm^{-1}. The frequency range
143 of spectra obtained from the polyethylene pellets was 50-500 cm^{-1}, with an instrumental resolution of 4
144 cm^{-1}. Individual spectra were merged to produce the complete spectra shown in Figure 1 using
145 OPUS/IR (software of Bruker Analytische Messtechnik GmbH) by matching up sections in the region
146 ~200-400 cm^{-1} where they overlap.

147

148 **Quantitative analysis of primary spectra**

This is the peer-reviewed, final accepted version for American Mineralogist, published by the Mineralogical Society of America.
The published version is subject to change. Cite as Authors (Year) Title. American Mineralogist, in press.
DOI: https://doi.org/10.2138/am-2023-9197. http://www.minsocam.org/

Rather than following the conventional approach of identifying individual absorption peaks and assigning their symmetries, the objective of the quantitative analysis presented here was to extract spectral parameters that relate specifically to the structural state and thermodynamic evolution of anorthite with respect to Al/Si order. This analysis was undertaken on the original, unmerged spectra, following the methodologies set out in Atkinson et al. (1999).

Three sections of the spectra were selected for peak fitting on the basis that they showed the emergence of peaks as the degree of Al/Si order increased. The emerging peaks included a pair in the interval 300-320 cm^{-1} (Fig. 2a, b) and another pair in the interval 460-500 cm^{-1} (Fig. 2c, d). For each pair, the area under a wider frequency interval was first normalised so as to minimise the influence of any slight variations of the concentration of sample in the pellets or of background levels in the spectrometers. This reduced scatter but did not change the trend shown by the same analysis of the original, un-normalised, spectra. Figure 3 illustrates six fits using Lorentzian profiles for individual peaks in the frequency interval ~260-340 cm^{-1}, including shoulders of the peaks to either side of the group of interest in order to obtain a realistic background. The frequencies, $\omega_{1,320}$, $\omega_{2,320}$, and line widths, $\Gamma_{1,320}$, $\Gamma_{2,320}$, of the two peaks had uncertainties from the fits on the order of 0.2 cm^{-1} (Salje et al. 1989) for most of the spectra. The uncertainties were greater than this for spectra from the least ordered samples. Areas of all the Lorentzian peaks within the group were summed to give a single overall intensity, I_{320}. This value had less scatter than the individual peak intensities as the relative sizes of the peaks within the group were not well constrained by the fitting procedure. The same procedure as set out above for the pair of peaks in the interval 300-320 cm^{-1} was used to determine values of frequencies, $\omega_{1,470}$, $\omega_{2,470}$, width, $\Gamma_{1,470}$, $\Gamma_{2,470}$, and combined intensity, I_{470}, of the two peaks between 460 and 500 cm^{-1} in Figure 2c,d.

The third focus of peak fitting was on an absorption peak with frequency close to 602 cm^{-1}, using the same approach as for the peaks near 320 and 470 cm^{-1}. By comparison with spectra from natural samples across the plagioclase solid solution (Atkinson et al. 1999) and the temperature dependence of

This is the peer-reviewed, final accepted version for American Mineralogist, published by the Mineralogical Society of America.
The published version is subject to change. Cite as Authors (Year) Title. American Mineralogist, in press.
DOI: https://doi.org/10.2138/am-2023-9197. http://www.minsocam.org/

spectra through the $I\bar{1} \leftrightarrow P\bar{1}$ transition in anorthite (Redfern and Salje 1992), this peak emerges most clearly when the crystals have $P\bar{1}$ symmetry. It is not visible in the spectrum from ANC19 (0.25 hours at 1100 °C), but developed with increasing intensity in the kinetic series (Fig. 1a) and is visible in all spectra for the equilibrium series (Fig. 1b). It can also be seen in Figure 1 of Atkinson et al. (1999) which includes spectra from natural samples with compositions in the range ~An_{71}-An_{100} and heat treated natural samples in the range ~An_{78}-An_{100}. In the stack of spectra shown for Monte Somma anorthite as a function of temperature in Figure 2 of Redfern and Salje (1992), it emerges as an increasingly distinct peak below ~700 K, ahead of the $I\bar{1} \leftrightarrow P\bar{1}$ transition at 515 ± 5 K.

Following the principles set out in Salje et al. (2000) and the approach of Atkinson et al. (1999) for analysing essentially the same groups of absorption peaks in spectra from natural plagioclase samples, the autocorrelation function was used to obtain an effective average linewidth for three different segments of the spectra: 270-450 cm^{-1}, 450-800 cm^{-1}, and 800-1500 cm^{-1}. These have been assigned labels $\Delta corr_{350}$, $\Delta corr_{600}$ and $\Delta corr_{1000}$, respectively. Δcorr values in Atkinson (1999) for natural samples were for frequency ranges 260-530, 515-830, 820-1400 cm^{-1}.

RESULTS

Primary spectra shown in Figure 1 closely resemble those reported previously from natural plagioclase samples (Salje et al. 1989; Redfern and Salje 1992; Atkinson et al. 1999). Low symmetry and large unit cell sizes result in multiple overlapping peaks with peak frequency variations, line widths, intensities and line broadening parameters that are sensitive to the degree of Al/Si order.

Figure 4 contains data for ω and Γ from fitting of the emerging peaks with frequencies near 320 and 470 cm^{-1} in Figure 2 and near 600 cm^{-1} in Figure 1. The kinetic and equilibrium series exhibit a well-defined trend of varying peak widths and almost no change in peak frequencies, with overlap for samples which contained type-b reflections in electron diffraction patterns ($I\bar{1}$ structure). There is no obvious break in slope at the point where type-e reflections gave way to type-b reflections. Data points

for ANC19, the sample with the lowest degree of Al/Si order, plot off the main trends but are relatively poorly constrained by the fitting procedure because the individual peaks were only weakly resolved in the primary spectra. Variations in peak widths correlate with changes in other parameters extracted from the spectra, such as peak intensities (Figure 5).

Each of the autocorrelation parameters $\Delta corr_{350}$, $\Delta corr_{600}$, and $\Delta corr_{1000}$, including those for ANC19, decreases systematically with increasing Al/Si order. $\Delta corr_{350}$, $\Delta corr_{600}$ correlate linearly with each other (Fig. 6a). Comparison of $\Delta corr_{350}$ and $\Delta corr_{600}$ with $\Delta corr_{1000}$ shows data points for the most ordered sample (which gave sharp type-c and type-d reflections) as deviating from a linear correlation (Fig. 6b). Figure 6c shows that decreasing $\Delta corr$ values correlate in a nonlinear manner with fitted peak widths, and that the nonlinearity increases with increasing order.

Line broadening parameters, Γ and $\Delta corr$, provide measures of the local heterogeneity within each sample via the spread of frequencies of specific absorption modes on the phonon length scale. A measure of the changes in Al/Si order averaged over a longer length scale, corresponding to at least the coherence length of X-ray diffraction, and hence to the macroscopic order parameter(s), is provided by the scalar strain, ε_s. $\Delta corr$ values display a nonlinear dependence on ε_s (Fig. 7a), but Γ for the peak near 600 cm^{-1} has a linear dependence (Fig. 7b). Data in Figure 7 taken from Atkinson et al. (1999) and Atkinson (1999) for two natural samples of anorthite before and after being heat treated at 1300 ºC or 1360 ºC have been added and are consistent with the overall pattern of correlations.

DISCUSSION

The clear outcome from analysing IR spectra from synthetic anorthite samples in this way is that the dominant influence of Al/Si disorder is seen as broadening of absorption peaks. In direct contrast, peak frequencies change very little through the full sequence of metastable states from those with the weakest development of incommensurate ordering through to equilibrium degrees of order based on the

This is the peer-reviewed, final accepted version for American Mineralogist, published by the Mineralogical Society of America.
The published version is subject to change. Cite as Authors (Year) Title. American Mineralogist, in press.
DOI: https://doi.org/10.2138/am-2023-9197. http://www.minsocam.org/

$I\bar{1}$ structure. ε_s represents the total long range elastic relaxation of the structure which occurs when more or less rigid AlO_4 and SiO_4 tetrahedra arrange themselves in crystals of anorthite such that, in the limit, there are no remaining Al-O-Al linkages. If ordering is incomplete, the net macroscopic strain, as defined with respect to the disordered state, is less and local distortions where the arrangements of adjacent tetrahedra do not conform to Al-avoidance occur instead. Line broadening parameters obtained from the IR spectra provide a view of the resulting local strain heterogeneity depending on the length scale of the phonons being sampled. As noted in the introduction above, these lengths scales are not well defined but are likely to be in the range ~10-100 Å. In this case, the observed Δcorr variations are indicative of local structural heterogeneity on a scale of at least ~1-5 unit cells

Hard modes and two order parameters

A conventional expectation of hard mode spectroscopy is that changes in peak widths, peak frequencies and peak intensities will scale, in lowest order, with the square of the order parameter (Salje 1992, 1994; Salje and Bismayer 1997). If this was simply Q_{od} for Al/Si ordering accompanying the change in macroscopic symmetry $C\bar{1} \rightarrow I\bar{1}$, each of the parameters, ω, Γ, Δcorr and Intensity would be expected to vary linearly both with each other and with the macroscopic strain, since each would be expected to scale with Q_{od}^2. While there is a general correlation among the line broadening parameters and strain, the trends are not linear and a contributary factor to this must be that, in anorthite at room temperature, these parameters depend on both Q_{od}^2 for the $C\bar{1} \rightarrow I\bar{1}$ transition and Q_{displ}^2 for the $I\bar{1} \rightarrow P\bar{1}$ transition.

Samples with the highest degree of order display the most obvious deviations from linear relationships between spectral parameters. They also have changes in the intensity and sharpness of the type-c and type-d reflections arising from the displacive transition which indicate that they have the largest values of Q_{displ}. It is well understood that there is strong, biquadratic coupling between the two

This is the peer-reviewed, final accepted version for American Mineralogist, published by the Mineralogical Society of America.
The published version is subject to change. Cite as Authors (Year) Title. American Mineralogist, in press.
DOI: https://doi.org/10.2138/am-2023-9197. http://www.minsocam.org/

order parameters, ie with the form $\lambda Q_{\mathrm{od}}^2 Q_{\mathrm{displ}}^2$, where λ is the coupling coefficient (Salje 1987; Redfern and Salje 1987; Redfern et al. 1988; Redfern 1992). The linear relationship between Γ for the peak near 600 cm^{-1} and the scalar strain seen in Figure 7b implies that both record the two order parameters in the same proportion. Likewise, the linear relationship shown in Figure 6a implies that $\Delta corr_{350}$ and $\Delta corr_{600}$ also have a dependence on the same proportions of the two order parameters as each other. Non-linear relationships seen in Figures 6b,c and Figure 7a imply that the dependence of $\Delta corr_{1000}$ and Γ for peaks near 320 and 470 cm^{-1} depend on a combination of Q_{od}^2 and Q_{displ}^2 which differs from those of Γ for the 600 cm^{-1} peak, $\Delta corr_{350}$, $\Delta corr_{600}$ and ε_s. Some additional measure of the order parameters would be needed to separate these dependences quantitatively, however.

$I\bar{1} \rightarrow P\bar{1}$ transition

Due to biquadratic coupling, local variations in the degree of Al/Si order are necessarily accompanied by local variations in displacements relating to the $P\bar{1}$ structure. Although the degree of Al/Si order in the synthetic samples has not been determined directly, Q_{od} is known to vary between 0.92 for a natural metamorphic anorthite sample and 0.78 after equilibration at ~1535 ºC (Angel et al. 1990; Carpenter et al. 1990). The observation that samples with relatively high degrees of Al/Si disorder gave diffuse type-c and type-d reflections in electron diffraction patterns is consistent with the original observation by Bruno et al. (1976) that anorthite crystals quenched from ~1530 ºC did not have type-c and type-d reflections in single crystal X-ray diffraction patterns.

Salje (1987) considered that the length scale of correlated displacements of atoms on the basis of $P\bar{1}$ symmetry would be reduced to less than ~200 Å, as an estimate for the typical length scale of X-ray diffraction, by local strain heterogeneity arising from the introduction of Al/Si disorder. This would also cause the $I\bar{1} \rightarrow P\bar{1}$ transition to become smeared rather than occurring at a discrete temperature. Spontaneous strain data extracted from lattice parameters measured as a function of temperature for a

This is the peer-reviewed, final accepted version for American Mineralogist, published by the Mineralogical Society of America.
The published version is subject to change. Cite as Authors (Year) Title. American Mineralogist, in press.
DOI: https://doi.org/10.2138/am-2023-9197. http://www.minsocam.org/

sample equilibrated at 1302 ± 4 ºC did not show evidence of such smearing (Redfern 1992), but the effect of disordering was seen increasingly in spontaneous strains from lattice parameters collected as a function of pressure through the related transition as a function of pressure in crystals equilibrated at temperatures between ~1350 ± 5 ºC (Q_{od} = 0.87) and ~1533 ± 5 ºC (Q_{od} = 0.78) (Angel 1992, 1994). Confirmation of the local heterogeneity responsible for this behaviour has been provided by the IR spectroscopy results reported here.

Elastic strain heterogeneity and enthalpy

Figure 8 contains a compilation of Δcorr data for synthetic anorthites from the present study with data from Atkinson et al. (1999) and Atkinson (1999) plotted as a function of composition. Dashed lines are guides to the eye illustrating linear extrapolation to An_{100} of fits to data in the range ~An_{20}-An_{60} for heat treated series samples which have $C\bar{1}$ symmetry. Each of the Δcorr parameters has the same pattern of a break in slope when $C\bar{1}$ members of the solid solution give way to $I\bar{1}$ members. Each also hasvalues for synthetic anorthites which spread between natural, ordered anorthite and the extrapolated limit for $C\bar{1}$ structures. When expressed simply in terms of these parameters alone, deviations from the trend for a solid solution with $C\bar{1}$ symmetry are clearly due to the Al/Si ordering.

Correlations between enthalpy and local strain heterogeneity from Δcorr for plagioclase feldspars were discussed in detail by Atkinson et al. (1999) and are confirmed in Figure 9. Figure 9a shows almost linear relationships between Δcorr and ΔH_{soln} for Al/Si ordering in anorthite, apart from the value of ΔH_{soln} for ANC19 which is considered to be lower than would be expected for the most disordered crystalline state due to the presence of a small amount of residual glass (Carpenter 1991b). Any non-linearity would be due predominantly to the additional contributions of Q^2_{displ} to Δcorr but might also include a slight dependence of the enthalpy of ordering on higher order terms than Q^2_{od} alone (Carpenter 1992). Figure 9b is the equivalent for ΔH_{soln} as a function of composition to the Δcorr

This is the peer-reviewed, final accepted version for American Mineralogist, published by the Mineralogical Society of America.
The published version is subject to change. Cite as Authors (Year) Title. American Mineralogist, in press.
DOI: https://doi.org/10.2138/am-2023-9197. http://www.minsocam.org/

295 variations shown in Figure 8. Just as with Δcorr, the spread of ΔH_{soln} values for synthetic anorthites is
296 between values for ordered anorthite and the extrapolated end member of a solid solution with $C\bar{1}$
297 symmetry.

298 Spectral parameters showing line broadening in anorthite clearly correlate with enthalpy changes
299 due to ordering, and the data in Figure 9b confirm the previous conclusion that deviations from ideality
300 in the enthalpy of mixing for the solid solution of plagioclase in "high" structural states arises from
301 Al/Si ordering in anorthite-rich compositions. The enthalpy of ordering in anorthite and anorthite-rich
302 compositions is also closely associated with the elimination of local strain heterogeneity.

303

304 **Structural evolution from incommensurate to commensurate ordering**

305 The initial Al/Si ordering scheme that develops in anorthite crystallised from chips of glass in air
306 displays characteristic features in diffraction patterns which mimic closely those of the incommensurate
307 structures in natural samples with intermediate compositions in the plagioclase solid solution
308 (Carpenter 1991a). NMR spectroscopy on the same samples has shown that changes with annealing
309 time occur by apparently continuous reductions in the number of Al-O-Al linkages (Phillips et al.
310 1992). Elimination of Al-O-Al linkages might conventionally be understood in terms of the long
311 established principle of Al-avoidance or Loewenstein's rule whereby Al in silicates avoids occupying
312 tetrahedral sites adjacent to others also occupied by Al. However, as discussed at length by Dove et al.
313 (1996), this view is simplistic because the Al/Si ordering transition temperature for some silicates is so
314 low that ordering does not occur even on a geological timescale.

315 At the length scale of phonons, between the coherence length of X-ray diffraction and the near
316 neighbour scale of NMR, local ordering in the incommensurate structure of anorthite evolving into that
317 of the $I\bar{1}$ structure is accompanied by elimination of local strain. On this basis, the driving force for
318 ordering comes from the need to minimise the elastic strain energy in structures where a disordered
319 configuration of more or less rigid AlO_4 and SiO_4 tetrahedra with different sizes cannot be

This is the peer-reviewed, final accepted version for American Mineralogist, published by the Mineralogical Society of America.
The published version is subject to change. Cite as Authors (Year) Title. American Mineralogist, in press.
DOI: https://doi.org/10.2138/am-2023-9197. http://www.minsocam.org/

accommodated in a given structure without introduction of local strain heterogeneity. The stable incommensurate arrangement of tetrahedra in intermediate plagioclase and the related metastable arrangement in incommensurate anorthite just provides one way in which AlO_4 and SiO_4 units can be arranged to reduce the local strain energy. At intermediate compositions it provides the lowest energy scheme, while ordering on the basis of the commensurate $I\bar{1}$ structure allows further elimination of the local strains in anorthite.

Advanced refinements of the structure of the e_1 form of the incommensurate structure in a sample with composition An_{51} from a metamorphic rock have revealed additional structural changes accompanying Al/Si ordering (Jin and Xu 2017). The modulation period of ~30 A for this sample is within the length scale over which local strain fields related to the arrangements of AlO_4 and SiO_4 tetrahedra would extend. Adjustments of Na and Ca positions in response to relaxations of the local heterogeneity provide additional stabilisation of the incommensurate structure and involve a small degree of chemical segregation.

Finally, a high degree of short range order in the $C\bar{1}$ solid solution provides further demonstration of the fact that the three dimensional feldspar framework structure is singularly unsuitable for accommodating disordered arrangements of AlO_4 and SiO_4 tetrahedra without introducing large local strain fields.

Strain and elasticity in thermodynamic mixing models of silicate solid solutions

A defining role for local and macroscopic strain energies fits with understanding of the mixing properties of silicate solid solutions more widely. The two dominant properties controlling excess enthalpies of mixing on cation sites are the difference in size of the substituting ions and the elastic constants of the host crystal (Carpenter and Boffa Ballaran 2001; Tarantino et al. 2003). Particularly striking in this context is the jadeite ($NaAlSi_2O_6$) – augite ($Ca(Mg,Fe)Si_2O_6$) solid solution for which changes in Δcorr and ΔH_{soln} due to ordering of cations at intermediate compositions are exactly the

345 reverse of changes due to mixing of the disordered structure (Boffa Ballaran et al. 1998; Carpenter and
346 Boffa Ballaran 2001). As in the case of anorthite presented in the present paper, cation ordering
347 involves the conversion of local strain fields into a single, homogeneous macroscopic strain. It is
348 unlikely that pairwise atomic interaction models will be able to mimic this behaviour unless they
349 include the longer range strain relaxations.
350
351 **Elastic moduli for trace element partitioning between plagioclase crystals and silicate melt**
352 As discussed above for cation ordering and solid solution formation, the model of Blundy and Wood
353 (1984) for partitioning of trace elements between crystals and melt in silicate systems attributes the
354 energies involved to the elastic strain energy associated with substitution of one cation by another with
355 a different size. It depends on an effective Young's modulus for the site on which the substitution
356 occurs and this, in turn, is related to the Young's modulus of the bulk crystal. Mutch et al. (2022)
357 recently reviewed treatments of the partitioning of Mg^{2+} between plagioclase crystals and melt that had
358 included a smooth variation of properties with composition across the plagioclase solid solution. They
359 found that a better match with experimental data was obtained if an inflection point was included in the
360 composition dependence of the partition coefficient at temperatures and compositions corresponding to
361 the locus of the $C\bar{1} \leftrightarrow I\bar{1}$ transition. They also noted, however, that the values of bulk and shear moduli
362 reported by Brown et al. (2016) do not show any equivalent reversal in trends at anorthite-rich
363 compositions. Instead, they attributed the change in partitioning behaviour to a crossover from
364 preferential location of Mg^{2+} in M sites to preferential occupancy of tetrahedral sites across the $C\bar{1} \leftrightarrow$
365 $I\bar{1}$ boundary.
366 No single dataset is yet available for the Young's modulus of plagioclase crystals with different
367 degrees of Al/Si order corresponding to those that would develop at the pressure/temperature
368 conditions in the earth where crystals would coexist with melt. Shear and bulk moduli given by Brown
369 et al. (2016) were all obtained at room temperature using natural crystals from a mixture of geological

This is the peer-reviewed, final accepted version for American Mineralogist, published by the Mineralogical Society of America.
The published version is subject to change. Cite as Authors (Year) Title. American Mineralogist, in press.
DOI: https://doi.org/10.2138/am-2023-9197. http://www.minsocam.org/

environments. As such, they are unlikely to reveal any systematic dependence of the elastic moduli on the degree of Al/Si order. An additional consideration is that the $I\bar{1} \rightarrow P\bar{1}$ transition must necessarily contribute to changes in elastic properties of anorthite-rich crystals measured at room temperature, as opposed to the temperatures at which trace element partitioning occurs. The influence of coupling between Q_{displ} and strain has not been determined but would give changes in moduli with the form typical of a co-elastic transition, ie not dissimilar from the pattern shown through the $\alpha \leftrightarrow \beta$ transition in quartz (Carpenter et al. 1998; Carpenter and Salje 1998) and on the order of a few percent to low tens of percent. On the other hand, the compilation of data shown in Figure 10 for the bulk modulus determined by single crystal X-ray diffraction measurements as a function of pressure is sufficient to suggest there is indeed a significant change in elastic properties associated with the $C\bar{1} \leftrightarrow I\bar{1}$ transition. Data for crystals with different compositions were taken from Figure 5 of Brown et al. (2016) and data for anorthite crystals with different degrees of Al/Si order were taken from Table 2 of Angel (1994).

The data for K_o in Figure 10 show two overlapping trends: increasing values with increasing anorthite content and decreasing values with increasing Al/Si disorder. Information about the disordering is provided by the observation of a displacive phase transition, $P\bar{1} \rightarrow I\bar{1}$, with increasing pressure (Angel et al. 1988, 1989; Angel 1988, 1992, 1994). Although the high pressure structure of anorthite with $I\bar{1}$ symmetry has some subtle differences from the $I\bar{1}$ structure at high temperatures, K_o for the former varies systematically according to the temperature at which the crystals had previously been annealed. Anorthite crystals equilibrated at 1533 ± 5 °C (Q_{od} = 0.78) gave K_o = 66.3 ± 1.7 GPa, crystals equilibrated at 1350 ± 5 °C (Q_{od} = 0.87) gave K_o = 77.1 ± 1.7 GPa, and crystals equilibrated during slow cooling in nature (Q_{od} = 0.92) gave K_o = 88.6 ± 3.7 GPa (Angel 1994). A similar dependence of K_o on Q_{od} for other plagioclase crystals with $I\bar{1}$ symmetry would decrease with reducing anorthite content towards the $C\bar{1}/I\bar{1}$ boundary.

This is the peer-reviewed, final accepted version for American Mineralogist, published by the Mineralogical Society of America.
The published version is subject to change. Cite as Authors (Year) Title. American Mineralogist, in press.
DOI: https://doi.org/10.2138/am-2023-9197. http://www.minsocam.org/

For reasons of stoichiometry, full ordering on the basis of $C\bar{1}$ symmetry is restricted to pure albite, and members of the solid solution with compositions that fall on the $C\bar{1}$ side of the $C\bar{1}/I\bar{1}$ line do not show the same extent of Al/Si order variation. The small break in slope at ~50 % An for K_o of natural samples in Figure 10 is not outside realistic experimental uncertainty limits but would be amplified significantly if the anorthite-rich crystals had a degree of Al/Si disorder. The expectation, therefore, is that for temperatures corresponding to those at which plagioclase crystals coexist with a basaltic liquid there should be a maximum in K_o half way across the solid solution. In the Blundy and Wood model, such a break in slope of bulk modulus with composition would contribute to the pattern of partition coefficients for Mg^{2+} between plagioclase and melt reported by Mutch et al. (2022), though the magnitude of the contribution remains undefined.

In the absence of a more comprehensive data set for crystals with wide ranges of composition and order, variations of spectral parameters such as $\Delta corr_{570}$ and $\Delta corr_{1000}$ can provide a prediction of the form of variations of K_o because of their sensitivity to Al/Si ordering. The relationship is explicit for anorthite because observed values of K_o for both the high pressure $I\bar{1}$ structure and the $P\bar{1}$ structure vary linearly with Q_{od}^2, due to a coupling term between spontaneous strain, e, and Q_{od} of the form $\lambda e^2 Q_{od}^2$ (Carpenter 2006). On this basis, the data in Figure 8 imply that the dependence of K_o on the degree of Al/Si order should be greatest for pure albite and pure anorthite and smallest for crystals with compositions in the range ~20-50 % An. The sensitivity of K_o to Q_{od} should increase with anorthite content and there should be a non-linear variation of K_o with composition for suites of crystals which have crystallised at more or less the same temperature. The same arguments apply to the shear modulus but there are currently no data available to separate any influence of the $I\bar{1} \rightarrow P\bar{1}$ transition from the room-temperature data of Brown et al. (2016). In order to correlate the real influence of changing bulk and shear moduli on trace element partitioning, it will be necessary to determine their values for

This is the peer-reviewed, final accepted version for American Mineralogist, published by the Mineralogical Society of America.
The published version is subject to change. Cite as Authors (Year) Title. American Mineralogist, in press.
DOI: https://doi.org/10.2138/am-2023-9197. http://www.minsocam.org/

samples with degrees of Al/Si order equilibrated at liquidus temperatures as measured at temperatures above the $I\bar{1} \rightarrow P\bar{1}$ transition.

A final consideration in this context is that, because there must be some degree of strain variation through twin walls in a crystal, partition coefficients between bulk crystal and melt must be different from those for partitioning between twin walls and melt. Changes in the concentration of cations have been seen at transformation twin walls in anorthoclase, for example (Hayward et al. 1998). Albite-rich crystals typically have a higher density of growth twins than An-rich crystals and this ought to influence the overall pattern of partitioning with composition. It remains to be determined whether the number of crystallographic sites on and immediately adjacent to twin walls, as a proportion of the total number of sites in a crystal, would be sufficient for this effect to be detectable.

CONCLUSIONS

Autocorrelation analysis of line broadening in IR powder absorption spectra from synthetic anorthite samples with a wide range of structural states has shown that the predominant effect of Al/Si ordering in the feldspar structure is to reduce local strain heterogeneity. Close correlation of line broadening parameters with calorimetric data has then shown that the enthalpy of ordering can be understood in terms of the accompanying reduction in elastic strain energy. Comparisons of line broadening parameters with calorimetric data for members of the plagioclase solid solution confirm the view that the thermodynamic mixing properties of plagioclase feldspars depend essentially on these order/disorder processes. Given that strain fields generate long ranging interactions within a structure, it follows that mean field models, such as Bragg Williams or Landau, should provide physically realistic descriptions of the overall thermodynamic behaviour. More generally, the Al-avoidance principle or Loewenstein's rule is expected to apply when the geometry of a structure does not allow relaxation of local strain effects arising from the difference in size of AlO_4 and SiO_4 tetrahedra but not when the geometry allow local strains to be eliminated by relaxation. The same constraints of strain

and elasticity that apply to solid solution formation also apply to incorporation of trace elements and, hence, to partition coefficients.

IMPLICATIONS

Key outcomes are firstly that the dominant effect of Al/Si disordering in anorthite is to give rise a high degree of local strain heterogeneity, secondly that Al-avoidance can be understood completely in terms of the need to minimise the strain associated with accommodating the different sizes of relatively rigid AlO_4 and SiO_4 tetrahedra in a framework structure, and thirdly that the reduction of the local heterogeneity with increasing order correlates with changes in macroscopic strain and enthalpy. While activity models of the plagioclase solid solution can skate over these effects, any physically accurate description of the structures will need to incorporate the effects of strain relaxation on a scale of at least a few unit cells. This treatment completes the picture of strain and elasticity as being the predominant factors in determining the properties of minerals which undergo displacive transitions, such as in stishovite (Carpenter et al. 2000), the driving mechanism for cation ordering transitions, such as in omphacite (Boffa Ballaran et al. 1998) and anorthite (this study), the mixing behaviour of solid solutions such as feldspars, pyroxenes, amphiboles and garnet (Carpenter and Boffa Ballaran 2001), and partitioning of trace elements such as in the Blundy-Wood model (Blundy and Wood 1994).

ACKNOWLEDGEMENTS AND FUNDING

Funding is acknowledged from St. John's College, Cambridge, (PhD studentship to AA), and from the Natural Environment Research Council of Great Britain (grant no. GR3/5547A to MAC for calorimetry).

REFERENCES CITED

Angel, R.J. (*1988*) High-pressure structure of anorthite. American Mineralogist, 73, 1114–1119.

466 Angel, R.J. (1992) Order-disorder and the high-pressure and $P\bar{1}$ - $I\bar{1}$ transition in anorthite. American
467 Mineralogist, 77, 923–929.
468 Angel, R.J. (1994) Feldspars at high pressure. In I. Parsons, Ed. Feldspars and their reactions, C421, p.
469 271–312. Kluwer Academic Publishers, Dordrecht.
470 Angel, R.J., Hazen, R.M., McCormick, T.C., Prewitt, C.T., and Smyth, J.R. (1988) Comparative
471 compressibility of end-member feldspars. Physics and Chemistry of Minerals, 15, 313–318.
472 Angel, R.J., Redfern, S.A.T., and Ross, N.L. (1989) Spontaneous strain below the $I\bar{1}$ - $P\bar{1}$ transition in
473 anorthite at pressure. Physics and Chemistry of Minerals, 16, 539–544.
474 Angel, R.J., Carpenter, M.A., and Finger, L.W. (1990) Structural variation associated with
475 compositional variation and order-disorder behavior in anorthite-rich feldspars. American
476 Mineralogist, 75, 150–162.
477 Atkinson, A. (1999) The role of strain in incommensurate plagioclase feldspars. Ph.D. thesis,
478 University of Cambridge, UK.
479 Atkinson, A., Carpenter, M.A., and Salje, E.K.H. (1999) Hard mode infrared spectroscopy of
480 plagioclase feldspars. European Journal of Mineralogy, 11, 7–21.
481 Benisek, A., Kroll, H., and Cemic, L. (2004) New developments in two-feldspar thermometry.
482 American Mineralogist, 89, 1496–1504.
483 Benisek, A., Dachs, E., and Kroll, H. (2010) A ternary feldspar-mixing model based on calorimetric
484 data: development and application. Contributions in Mineralogy and Petrology, 160, 327–337.
485 Bersani, D., Aliatis, I., Tribaudino, M., Mantovani, L., Benisek, A., and Carpenter, M.A. (2018)
486 Plagioclase composition by Raman spectroscopy. Journal of Raman Spectroscopy, 49, 684-698.
487 Blundy, J., and Wood, B. (1984) Prediction of crystal-melt partition coefficients from elastic moduli.
488 Nature, 372, 452–454.

Boffa Ballaran, T., Carpenter, M.A., Domeneghetti, M.C., Salje, E.K.H., and Tazzoli, V. (1998) Structural mechanisms of solid solution and cation ordering in augite-jadeite pyroxenes: II. A microscopic perspective. American Mineralogist, 83, 434–443.

Brown, J.M., Angel, R.J., and Ross, N.L. (2016) Journal of Geophysical Research: Solid Earth, 121, 663–675.

Bruno, E., Chiari, G., and Facchinelli, A. (1976) Anorthite quenched from 1530 ºC. I. Structure refinement. Acta Crystallographica B, 32, 3270–3280.

Carpenter, M.A. (1991a) Mechanisms and kinetics of Al/Si ordering in anorthite, I: Incommensurate structure and domain coarsening. American Mineralogist, 76, 1110–1119.

Carpenter, M.A. (1991b) Mechanisms and kinetics of Al/Si ordering in anorthite, II: energetics and a Ginzburg-Landau rate law. American Mineralogist, 76, 1120–1133.

Carpenter, M.A. (1992) Equilibrium thermodynamics of Al/Si ordering in anorthite. Physics and Chemistry of Minerals, 19, 1–24.

Carpenter, M.A. (1994) Subsolidus phase relations of the plagioclase feldspar solid solution. In I. Parsons, Ed. Feldspars and their reactions, C421, p. 221–269. Kluwer Academic Publishers, Dordrecht.

Carpenter, M.A., and Boffa Ballaran, T. (2001) The influence of elastic strain heterogeneities in silicate solid solutions. European Mineralogical Union Notes in Mineralogy, 3, 155–178.

Carpenter, M.A. (2002) Microscopic strain, macroscopic strain and the thermodynamics of phase transitions in minerals. European Mineralogical Union Notes in Mineralogy, 4, 311–346.

Carpenter, M.A. (2006) Elastic properties of minerals and the influence of phase transitions. American Mineralogist, 91, 229–246.

Carpenter, M.A., and Boffa Ballaran, T. (2001) The influence of elastic strain heterogeneities in silicate solid solutions. European Mineralogical Union Notes in Mineralogy, 3, 155–178.

513 Carpenter, M.A., and Ferry, J.M. (l984) Constraints on the thermodynamic mixing properties of
514 plagioclase feldspars. Contributions to Mineralogy and Petrology, 87, 138–148.
515 Carpenter, M.A., and Salje, E.K.H. (1998) Elastic anomalies in minerals due to structural phase
516 transitions. European Journal of Mineralogy, 10, 693–812.
517 Carpenter, M.A., McConnell, J.D.C., and Navrotsky, A. (1985) Enthalpies of ordering in the
518 plagioclase feldspar solid solution. Geochimica et Cosmochimica Acta, 49, 947–966.
519 Carpenter, M.A., Salje, E.K.H., Graeme-Barber, A., Wruck, B., Dove, M.T., and Knight, K.S. (1998)
520 Calibration of excess thermodynamic properties and elastic constant variations associated with the α
521 ↔ β phase transition in quartz. American Mineralogist, 83, 2–22.
522 Carpenter, M.A., Angel, R.J., and Finger, L.W. (1990) Calibration of Al/Si order variations in
523 anorthite. Contributions to Mineralogy and Petrology, 104, 471–480.
524 Carpenter, M.A., Boffa Ballaran, T., and Atkinson, A.J. (1999) Microscopic strain, local structural
525 heterogeneity and the energetics of silicate solid solutions. Phase Transitions, 69, 95–109.
526 Carpenter, M.A., Hemley, R.J., and Mao, H.K. (2000) High-pressure elasticity of stishovite and the
527 $P4_2/mnm$ - *Pnnm* phase transition. Journal of Geophysical Research, 105, 10807–10816.
528 Dove, M.T., Thayaparam, I.S., Heine, V., and Hammonds, K.D. (1996) The phenomenon of low Al-Si
529 ordering temperatures in aluminosilicate framework structures. American Mineralogist, 81, 349–
530 362.
531 Dubacq, B. (2022) Thermodynamics of ordering and mixing in plagioclase feldspars: atomistic
532 modelling in favour of Landau theory. Contributions to Mineralogy and Petrology, 177, 102.
533 Eshelby, J.D. (1957) The determination of the elastic field of an ellipsoidal inclusion, and related
534 problems. Proceedings of the Royal Society of London A, 241, 376–396.
535 Ghiorso, M. (1984) Activity/composition relations in the ternary feldspars. Contributions to
536 Mineralogy and Petrology, 87, 282–296.

537 Hayward, S.A., Salje, E.K.H., and Chrosch, J. (1998) Local fluctuations in feldspar frameworks.
538 Mineralogical Magazine, 62, 639–645.
539 Holland, T.J.B., and Powell, R. (1992) Plagioclase feldspars: activity-composition relations based upon
540 Darken's quadratic formalism and Landau theory. American Mineralogist, 77, 53–61.
541 Holland, T.J.B., Green, E.C.R., and Powell, R. (2022) A thermodynamic model for feldspars in
542 $KAlSi_3O_8$–$NaAlSi_3O_8$–$CaAl_2Si_2O_8$ for mineral equilibrium calculations. Journal of Metamorphic
543 Geology, 40, 587–600.
544 Jin, S., and Xu, H. (2017) Solved: The enigma of labradorite feldspar with incommensurately
545 modulated structure. American Mineralogist, 102, 21–32
546 Mutch, E.J.F., Maclennan, J., and Madden-Nadeau, A.L. (2022) The dichotomous nature of Mg
547 partitioning between plagioclase and melt: implications for diffusion chronometry. Geochimica et
548 Cosmochimica Acta, 339, 173–189.
549 Namur, O., Charlier, B., Toplis, M., and Vander Auwera, J. (2012) Prediction of plagioclase-melt
550 equilibria in anhydrous silicate melts at 1-atm. Contributions to Mineralogy and Petrology, 163,
551 133–150.
552 Phillips, B.L., Kirkpatrick, R.J., and Carpenter, M.A. (1992) Investigation of short-range Al/Si order in
553 synthetic anorthite by ^{29}Si MAS NMR spectroscopy. American Mineralogist, 77, 484–494.
554 Redfern, S.A.T. (1992) The effect of Al/Si disorder on the $I\bar{1}$ - $P\bar{1}$ Co-elastic phase transition in Ca-
555 rich plagioclase. Physics and Chemistry of Minerals, 19, 246–254.
556 Redfern, S.A.T., and Salje, E. (1987) Thermodynamics of plagioclase II: Temperature evolution of the
557 spontaneous strain at the $I\bar{1}$ - $P\bar{1}$ phase transition in anorthite. Physics and Chemistry of Minerals,
558 13, 189–195.
559 Redfern, S.A.T., and Salje, E. (1992) Microscopic dynamic and macroscopic thermodynamic character
560 of the $I\bar{1}$ - $P\bar{1}$ phase transition in anorthite. Physics and Chemistry of Minerals, 18, 526–533.

561 Redfern, S.A.T., Graeme-Barber, A., and Salje, E. (1988) Thermodynamics of plagioclase III:
562 spontaneous strain at the $I\bar{1}$ - $P\bar{1}$ phase transition in Ca-rich plagioclase. Physics and Chemistry of
563 Minerals, 16, 157–163.
564 Salje, E. (1987) Thermodynamics of plagioclases I: Theory of the $I\bar{1}$ - $P\bar{1}$ phase transition in anorthite
565 and Ca-rich plagioclases. Physics and Chemistry of Minerals, 14, 181–188.
566 Salje, E.K.H. (1992) Hard mode spectroscopy: experimental studies of structural phase transitions.
567 Phase Transitions, 37, 83–110.
568 Salje, E.K.H. (1993) Phase transitions in ferroelastic and co-elastic crystals. Cambridge University
569 Press, Cambridge.
570 Salje 1994 Phase Transitions and Vibrational Spectroscopy in Feldspars. In I. Parsons, Ed. Feldspars
571 and their reactions, C421, p. 103–160. Kluwer Academic Publishers, Dordrecht.
572 Salje, E.K.H., and Bismayer, U. (1997) Hard mode spectroscopy: the concept and applications. Phase
573 Transitions, 63, 1–75.
574 Salje, E.K.H., Güttler, B., and Ormerod, C. (1989) Determination of the degree of Al, Si order Q_{od} in
575 kinetically disordered albite using hard mode infrared spectroscopy. Physics and Chemistry of
576 Minerals, 16, 576–581.
577 Salje, E.K.H., Carpenter, M.A., Malcherek, T., and Boffa Ballaran, T. (2000) Autocorrelation analysis
578 of infrared spectra from minerals. European Journal of Mineralogy, 12, 503–519.
579 Tarantino, S., Carpenter, M.A., and Domeneghetti, M.C. (2003) Strain and local heterogeneity in the
580 forsterite-fayalite solid solution. Physics and Chemistry of Minerals, 30, 495–502.
581 Xu, H., Buseck, P.R., and Carpenter, M.A. (1997) Twinning in synthetic anorthite: a transmission
582 electron microscopy investigation. American Mineralogist, 82, 125–130.
583

584 **FIGURE CAPTIONS**

585 **FIGURE 1.** (a) Merged infrared powder absorption spectra for the kinetic series of synthetic
586 anorthites. The annealing time for each sample is given in hours. All samples were heated at 1400 °C
587 except the lowest in the figure, which was heated at 1100 °C. (b) Merged spectra for the six
588 equilibrium samples. Annealing temperatures are given in °C. The spectrum of the sample equilibrated
589 at 1400 °C (with an annealing time of 1102 hours) has been also included in (a).
590
591 **FIGURE 2.** Details from infrared powder absorption spectra showing the emergence of new peaks at
592 around ~320 cm^{-1} for (a) the kinetic series and (b) the equilibrium series samples and at ~470 cm^{-1} for
593 (c) kinetic and (d) equilibrium samples. Note the change in intensity with time or annealing
594 temperature, reflecting changes in the degree of local order.
595
596 **FIGURE 3.** Examples of peak fitting of peak group at 300-320 cm^{-1} in spectra from synthetic anorthite
597 samples with different degrees of Al/Si order. Equilibrium series: (a) 850 °C, (b) 1400 °C, (c) 1536 °C.
598 Kinetic series: (d) 8.25 hrs, (e) 0.78 hrs, (f) 0.017 hrs. The fits are shown as solid lines and the original
599 spectra as dashed lines. The number of peaks used in the fit was arbitrary and does not necessarily
600 reflect the real number of modes present. The intensity of the peak group was obtained by the
601 summation of the areas of the peaks used in the fit.
602
603 **FIGURE 4.** Values of ω and Γ from peak fitting of selected peaks in primary spectra. Experimental
604 uncertainties are shown as ± 0.2 cm^{-1}, but uncertainties in the data for sample ANC19 are larger than
605 this. Data for samples with type-b reflections in the kinetic series generally overlap with data from the
606 equilibrium series. Any sensitivity of phonon frequencies to Al/Si order is clearly substantially less
607 than the sensitivity of line widths. (a) Peak with the higher frequency of the pair near 320 cm^{-1} in
608 Figure 2a,b. (b) The pair of peaks in Figure 2c,d. (c) Peak near 602 cm^{-1} in Figure 1.
609

FIGURE 5. Variation of linewidths, Γ, from peak fitting with respect to the integrated intensities of peaks. Γ values labelled as 320 were taken directly from the fits to the peak at ~322 cm^{-1}. Γ values labelled as 470 are averages for the two peaks at ~470 and ~490 cm^{-1}. I_{320} and I_{470} are the sum of intensities for each of the two pairs of peaks. Black lines are guides to the eye showing linear dependences between Γ and intensity.

FIGURE 6. Variations in parameters from autocorrelation analysis. $\Delta corr_{350}$, $\Delta corr_{600}$ and $\Delta corr_{1000}$ refer to frequency intervals 270-450 cm^{-1}, 450-800 cm^{-1}, and 800-1500 cm^{-1}, respectively. (a) Variations of $\Delta corr_{350}$ and $\Delta corr_{600}$ show essentially the same variation for the two frequency intervals. (b) $\Delta corr_{350}$ and $\Delta corr_{600}$ show linear correlation with $\Delta corr_{1000}$ apart from data points for the most ordered sample (equilibrated at 850 ºC). (c) Variations of Δcorr correlate with variations of peak width, Γ, from peak fitting but with increasing deviation from linearity with increasing Al/Si order. Γ470 is the average width of the two peaks near 470 cm^{-1} in Figures 2c,d. Γ600 is the width of the peak near 600 cm^{-1} in Figure 1.

FIGURE 7. Comparison of spectral parameters, which relate to variations in structural state at a phonon length scale, with scalar strain, which represents structural state variations on an X-ray length scale. Data for two natural samples of anorthite (An_{100}, Val Pasmeda; An_{98}, Monte Somma) are from Atkinson et al. (1999) and Atkinson (1999). "nat" refers to the natural samples without heat treatment, "heat treated" refers to the natural samples after heat treatment at 1300 ºC (An_{100}) and 1360 ºC (An_{98}), as set out in Carpenter et al. (1985). (a) Δcorr values show a non-linear correlation with ε_s. (b) Γ for the absorption peak near 600 cm^{-1} has a linear relationship with ε_s.

FIGURE 8. Variations of Δcorr values as a function of composition across the plagioclase feldspar solid solution. Data for natural and heated treated samples are from Atkinson et al. (1999) and Atkinson (1999). Heat treatment for samples represented by open triangles involved annealing in air at temperatures of ~1100-1400 ºC to induce a degree of Al/Si disorder consistent with $C\bar{1}$ symmetry in the composition range ~An0-An60 and $I\bar{1}$ ordering in the range ~An80-An100. The most An-rich samples had $P\bar{1}$ symmetry at room temperature. Dashed lines are guides to the eye from fitting to data for heat treated samples in the range ~An20-An60, with extrapolation to An100. Δcorr values for synthetic anorthite from the present study spread essentially between the value of the extrapolated straight line, $C\bar{1}$, and values for the most ordered natural anorthite samples.

FIGURE 9. Correlation of Δcorr data (coloured points = this study, black = from Atkinson et al. 1999 and Atkinson 1999) with Δ*H*soln data (Carpenter et al. 1985; Carpenter 1991b, 1992) for members of the plagioclase feldspar solid solution. ΔH_{soln} values for ANC19 were lower than would be expected for a disordered crystalline sample due to the presence of some residual glass from the starting material (Carpenter 1991b). Apart from these, there is a strong and almost linear correlation between Δcorr and ΔH_{soln} in (a). The pattern of ΔH_{soln} as a function of composition in (b) is almost exactly equivalent to the pattern of Δcorr values in Figure 8, with a spread between values for ordered samples and the extrapolated value for a solid solution with $C\bar{1}$ symmetry.

FIGURE 10. Values of the room pressure bulk modulus, K_o, of plagioclase feldspars determined by single-crystal high-pressure X-ray diffraction measurements at room temperature with the pressure dependence, K', set at 4. Values of Q_{od} refer to the degree of Al/Si order of anorthite samples equilibrated at different temperatures. Given that K_o of pure anorthite decreases markedly with decreasing Al/Si order and that crystals with less than ~50% anorthite cannot change to the same

extent, the break in slope at ~50% An would become more marked with increasing equilibration temperatures.

TABLES

TABLE 1. Synthesis and characterisation of two series of synthetic anorthite samples used in the present study. Data for structural states in terms of the presence of type-e or type-b reflections in electron diffraction patterns, values of scalar strain, ε_s, and values of heat of solution, ΔH_{soln}, are from Carpenter (1991b) (kinetic series) and Carpenter (1992) (equilibrium series). As reported in Carpenter (1991b), sample ANC19 contained some relict glass which accounted for its particularly low value of ΔH_{soln}.

Sample no.	Heat treatment		e or b reflections	Scalar strain, ε_s ($\pm 1\sigma$)	ΔH_{soln} (kJ.mole^{-1}, $\pm 1\sigma$)
	T (°C)	t (h)			
Disordered reference state					
ANC19	1102 ± 3	0.25	e	0	37.32 ± 0.96
Kinetic series					
ANC60	1385 ± 5	0.017	e	0.0039(2)	55.23 ± 0.63
ANC33	1392 ± 8	0.067	e	0.0047(2)	57.15 ± 0.46
ANC65	1398 ± 2	0.25	e	0.0054(2)	58.53 ± 0.75
ANC73	1400 ± 3	0.78	e+b	-	-
ANC38	1401 ± 1	1.5	b	0.0061(1)	59.75 ± 0.67
ANC39	1400	8.25	b	0.0065(2)	62.01 ± 0.33
ANC36	1400 ± 2	48	b	0.0066(2)	63.56 ± 63
ANC35	1402 ± 2	408	b	0.0069(2)	63.76 ± 1.09
Equilibrium series					
ANC69	1400 ± 2 then 1536 ± 1	361, 66	b	0.0054(2)	59.96 ± 0.84

ANC56	1400 ± 1 then 1500 ± 1	356, 301	b	0.0060(2)	61.97 ± 1.00
ANC48	1397 ± 1	1102	b	0.0070(2)	64.77 ± 0.88
ANC62	1392 ± 2 then 1300 ± 1	380, 1342	b	0.0073(2)	66.27 ± 0.50
ANC71	1402 ± 2 then 1202 ± 2	331, 2141	b	0.0076(2)	68.03 ± 0.75
ANC74/H2	1393 ± 6 then 850 ± 7, P_{H2O} = 750 bars	0.25, 3166	b	0.0082(2)	-

675
676
677
678
679
680
681
682
683

684 **FIGURES**

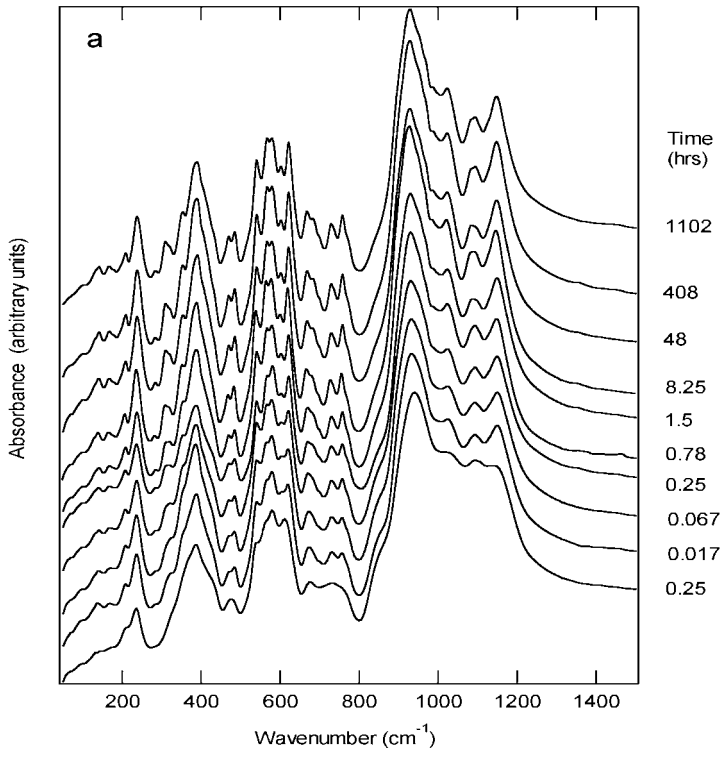

685

This is the peer-reviewed, final accepted version for American Mineralogist, published by the Mineralogical Society of America.
The published version is subject to change. Cite as Authors (Year) Title. American Mineralogist, in press.
DOI: https://doi.org/10.2138/am-2023-9197. http://www.minsocam.org/

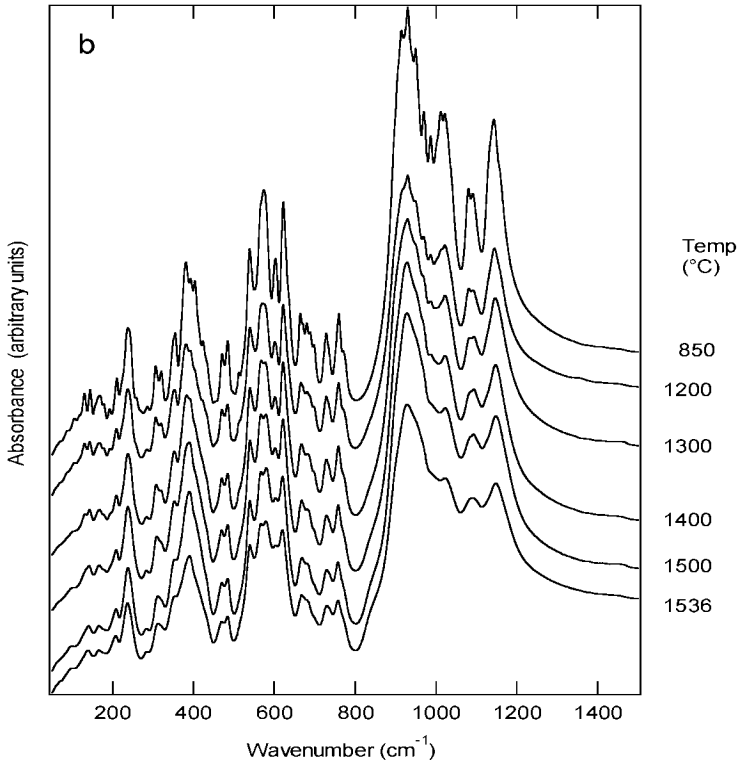

686

687 Figure 1

688

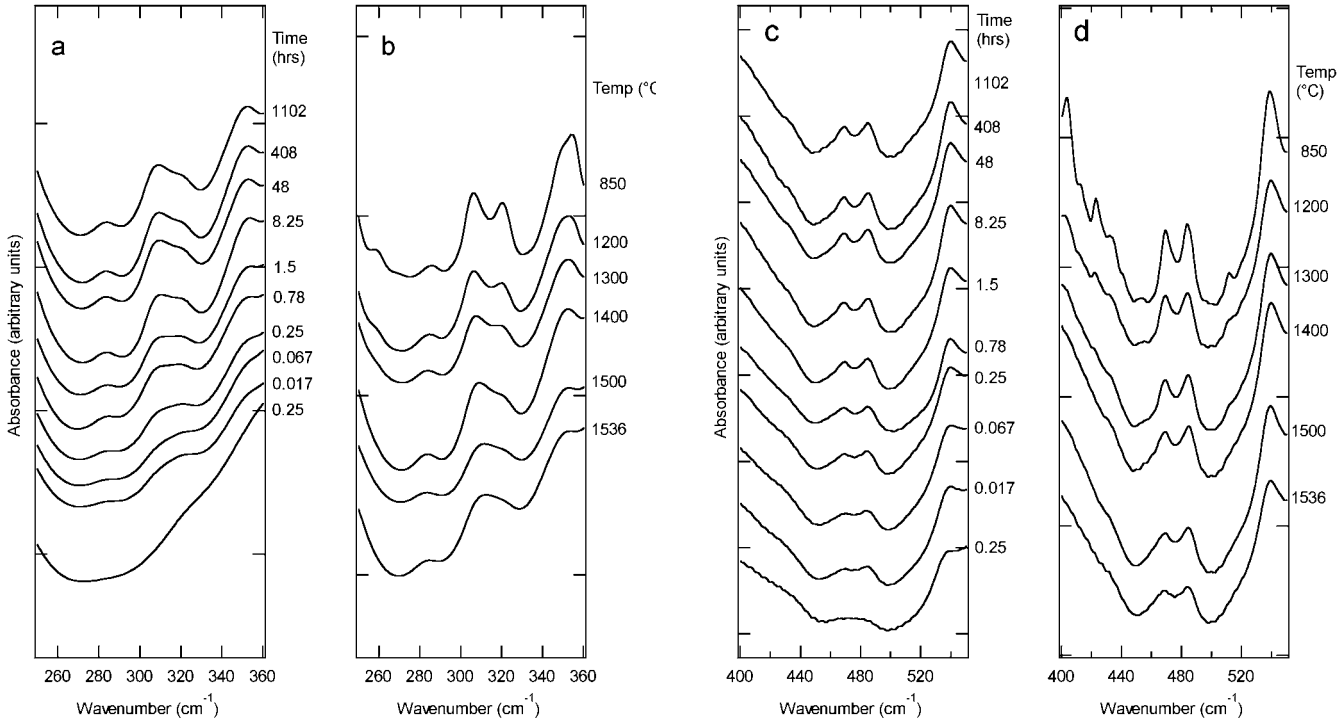

689 Figure 2

690

691

692

693

694

695

696

697

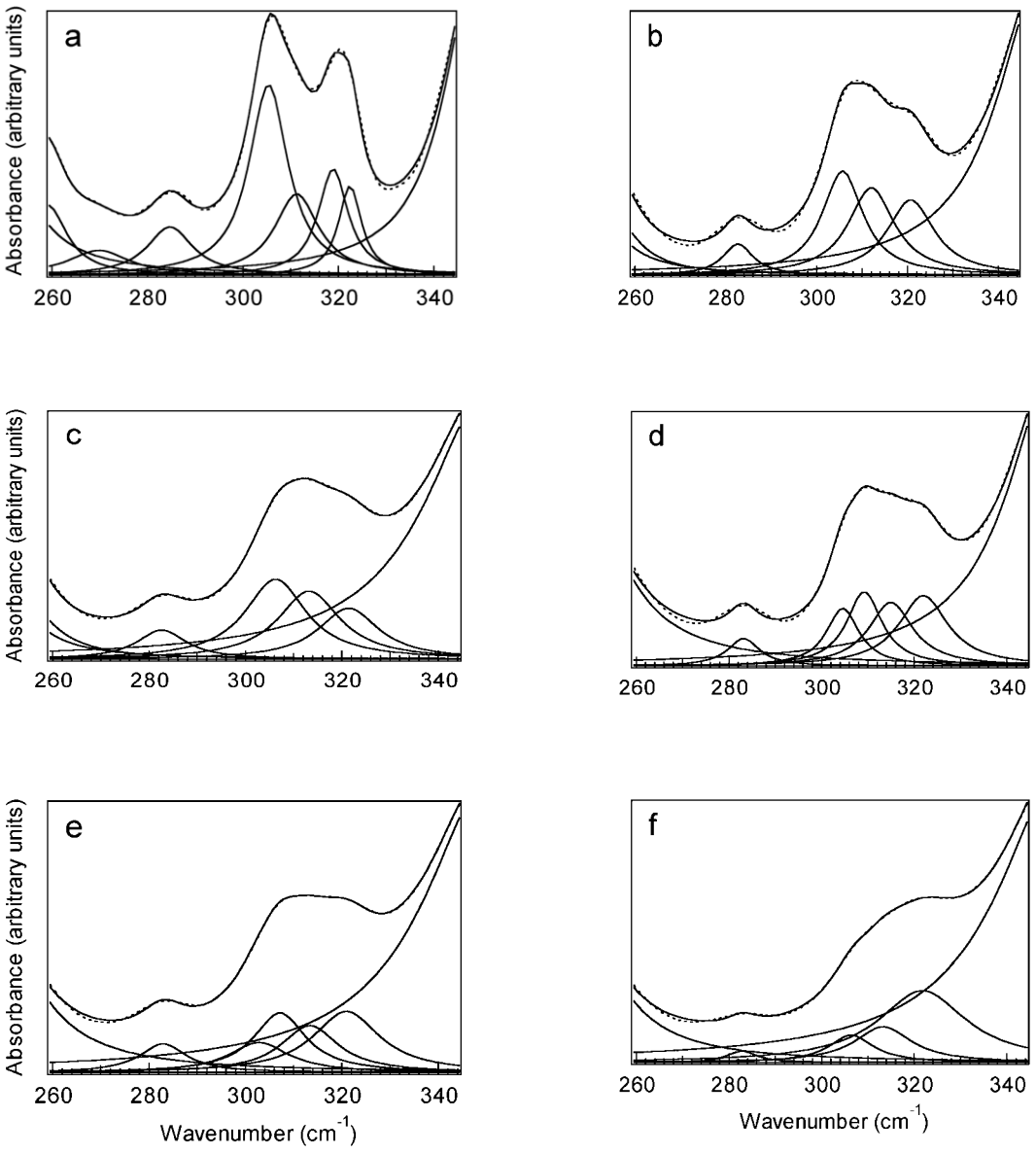

698 Figure 3

699

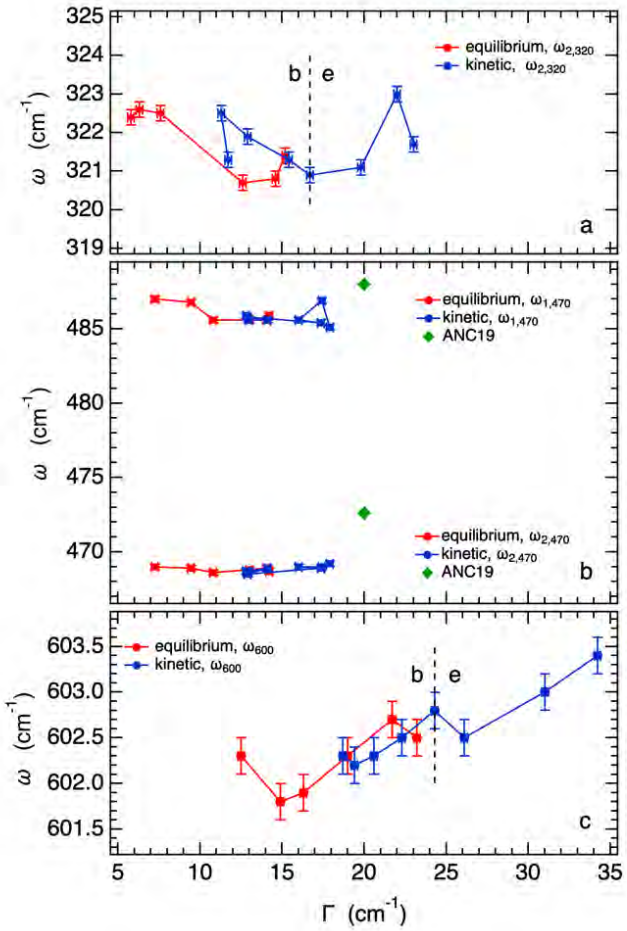

700

701 Figure 4

702

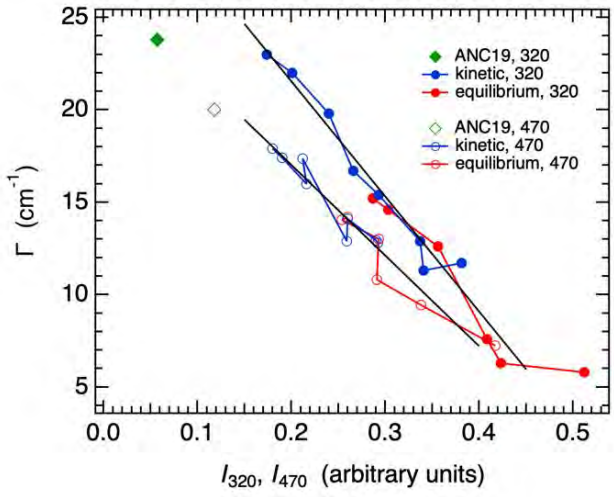

703

704 Figure 5

705

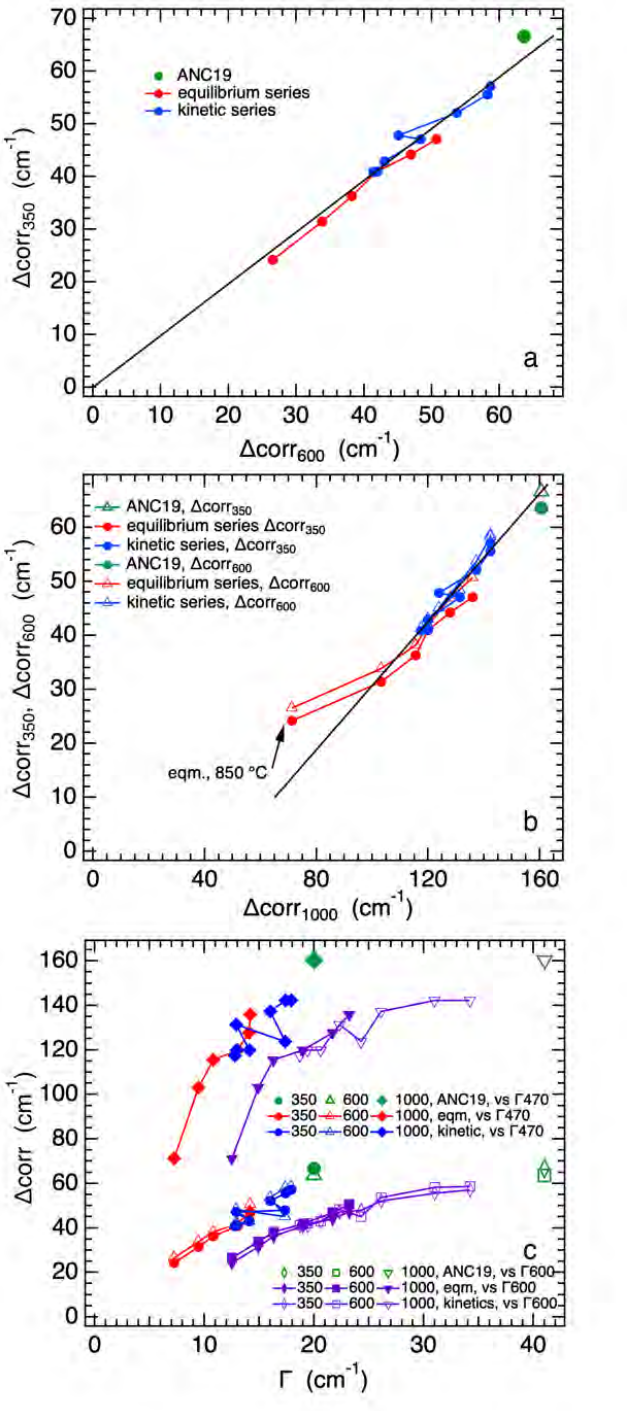

706

707 Figure 6

708

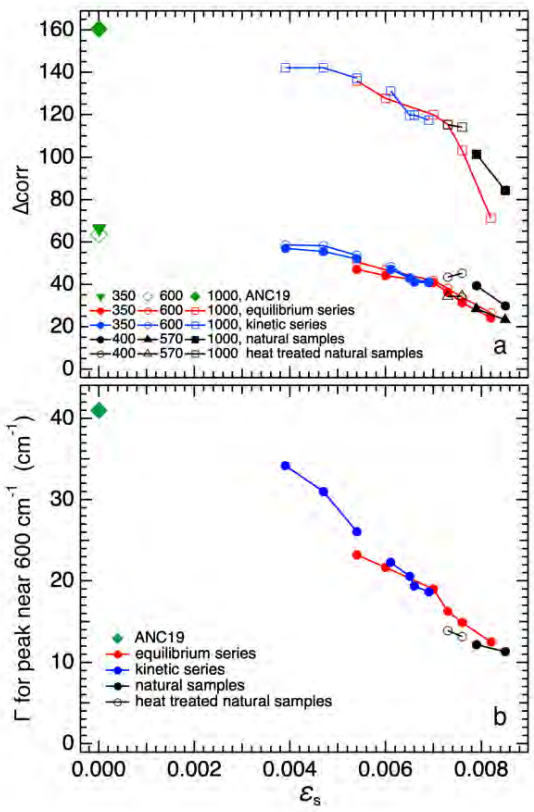

709

710 Figure 7

711

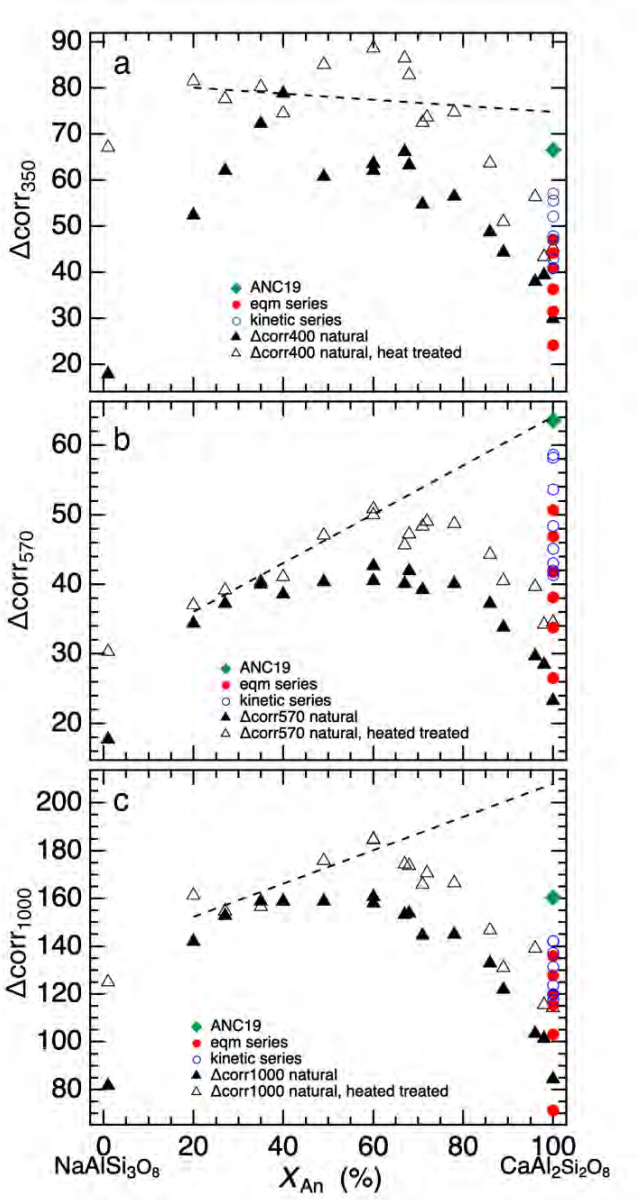

712

713 Figure 8

714

This is the peer-reviewed, final accepted version for American Mineralogist, published by the Mineralogical Society of America.
The published version is subject to change. Cite as Authors (Year) Title. American Mineralogist, in press.
DOI: https://doi.org/10.2138/am-2023-9197. http://www.minsocam.org/

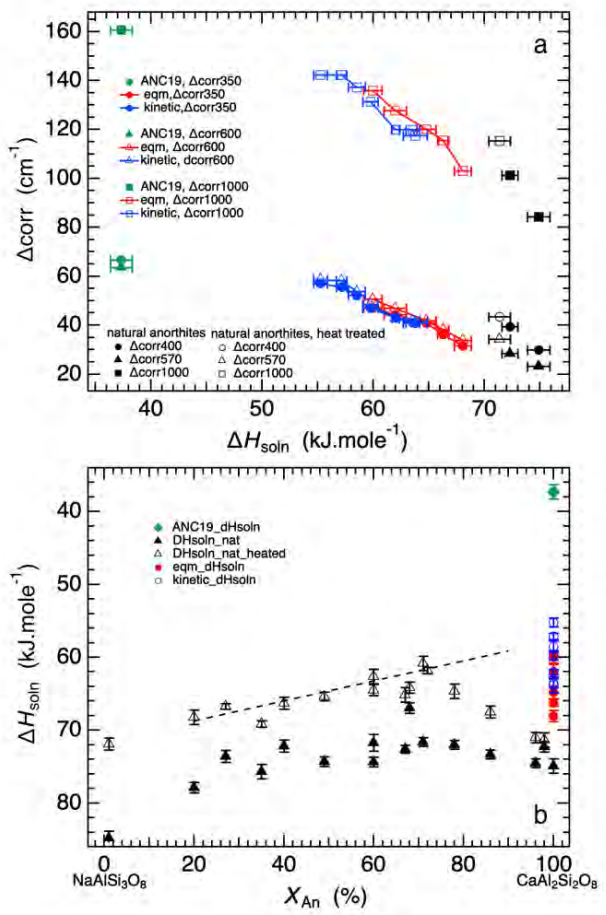

715

716 Figure 9

717

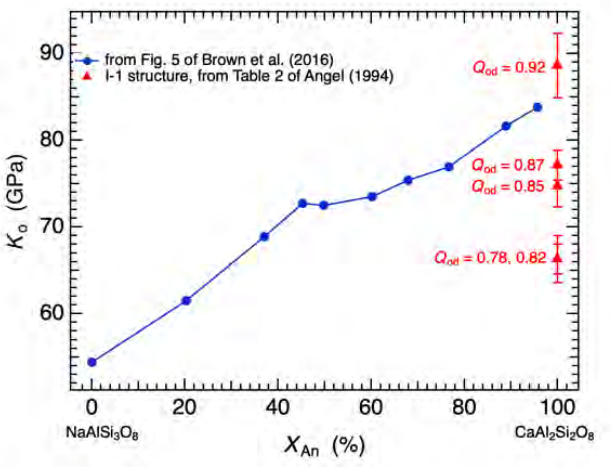

718

719 Figure 10